Received April 4, 2018, accepted May 1, 2018, date of publication May 10, 2018, date of current version June 5, 2018.

Digital Object Identifier 10.1109/ACCESS.2018.2834947

Array Synthesis for Optimal Microwave Power Transmission in the Presence of Excitation Errors

HUA-WEI ZHOU, XUE-XIA YANG, (Senior Member, IEEE), AND SAJJAD RAHIM

Key Laboratory of Specialty Fiber Optics and Optical Access Networks, Joint International Research Laboratory of Specialty Fiber Optics and Advanced Communication, Shanghai Institute of Advanced Communication and Data Science, Shanghai University, Shanghai 200444, China

Corresponding author: Xue-Xia Yang (yang.xx@shu.edu.cn)

This work was supported by the Natural Science Foundation of China under Grant 61271062 and Grant 61771300.

ABSTRACT Beam capture efficiency (BCE) is one key factor of the overall efficiency in a microwave power transmission (MPT) system. However, excitation errors of transmitting array are inevitable in practice, which always cause deviation of BCE from the designed one. In this paper, we propose a synthesis method of transmitting array for optimal MPT by using cooperatively coevolving differential evolution (CCDE) algorithm while considering excitation errors including amplitude errors and phase errors. Toward this purpose, a statistical analysis (SA) method is also presented to evaluate the achievable worst BCE in the presence of excitation errors. The tolerance of BCE against the random excitation errors is simulated by computer program, and the positions and nominal excitation amplitudes are both simultaneously optimized to improve the worst BCE. Simulated results show that the worst *BCE* is improved about 4% from 81% to 85% based on the SA-CCDE synthesis method for the excitation errors $(\sigma_\delta, \sigma_\Phi) = (0.1, 10^\circ)$, where δ_n denotes the amplitude error in percent and Φ_n represents the phase error.

INDEX TERMS Microwave power transmission, beam capture efficiency, array synthesis, excitation errors.

I. INTRODUCTION

Microwave power transmission (MPT) technology involves wirelessly transferring the electrical energy from transmitting antenna array to receiving antenna array by a microwave beam [1], [2]. It could be used for supplying high altitude airship, unmanned aerial vehicles, and so on [3], [4]. Beam capture efficiency (*BCE*) is the ratio of the captured power by the receiving array to the total radiated microwave power, and it is one key factor of overall efficiency for optimal MPT.

The highest dc to dc (dc-dc) overall efficiency of 54% in the history of MPT was proved by Dr. Brown in 1974 [5]. However, this culmination is hard to be achieved in a long-range MPT system. In 1975, an S-band MPT experiment at the range of 1.54 km was shown at the Venus Site of JPL's Goldstone Facility. The obtained rectifying efficiency was up to 80%, whereas the dc-dc efficiency was only 7% due to poor *BCE* of 11.7% [6]. Another MPT experiment was carried out by John Mankins in 2008, and the obtained *BCE* was less than 1/1000th of 1% since the size of the transmitting and receiving arrays were too small for efficient transfer over 148 km distance [7]. Therefore, the transmitting array should be designed to improve *BCE*, which is of great importance to efficient operation of MPT systems.

In recent years, many efforts have been devoted to the transmitting array synthesis for optimal MPT without considering excitation errors or position errors [8]–[17]. The theoretical optimal *BCE* (BCE^{opt}) and the corresponding optimal distribution across the transmitting array can be achieved by exploiting the discrete prolate spheroidal sequences [8] or by solving a generalized eigenvalue problem [9], [10]. To simplify the complexity of the feed network under the condition of keeping a high *BCE*, several weighting technologies have been proposed for the transmitting array including Isosceles Trapezoidal Distribution (ITD) [11], ITD with Unequal spacing [12], stepped amplitude distribution [13], and uniform amplitude distribution with unequal spacing [14]. The unconventional array can also realize the feed network simplification by clustered exciting strategy [15]. The sparsification of the transmitting array was also discussed in [15]–[17] with a high *BCE* via compressive sensing (CS), convex programming (CP), and the combination of the aforementioned two methods, respectively. Unfortunately, random errors are inevitable due to the accuracy of manufacture, which always cause deviation of *BCE* from the designed one. Nevertheless, [18], [19] just analyzed the tolerance of *BCE* against excitation phase errors and position errors, respectively. To the best of the authors' knowledge, the previous

array synthesis works for optimal MPT were focused on ideal situation.

In this work, we describe a synthesis method of the transmitting array for optimal MPT by using stochastic optimization algorithm in the presence of excitation errors including amplitude errors and phase errors. Toward this purpose, a statistical analysis (SA) method is also presented to analyze the tolerance of *BCE* against excitation errors. Due to high dimensions of this optimization problem, cooperatively coevolving differential evolution (CCDE) algorithm is considered [20]. The outline of this paper is organized as follows. Section II describes the SA method for tolerance analysis of *BCE* against excitation errors. Section III introduces the synthesis model and the optimization procedure of CCDE algorithm, and Section IV presents the numerical results. Finally, section V gives the concluding remarks.

II. TOLERANCE ANALYSIS OF *BCE* IN THE PRESENCE OF EXCITATION ERRORS

The formulas of *BCE* are derived by using SA method while considering excitation errors. Then based on these formulas, we can get the upper and lower bounds of *BCE*.

A. FORMULAS OF BCE WITH CONSIDERING EXCITATION ERRORS

As shown in Fig. 1, the transmitting array can be an arbitrary shaped array located in the XOY plane while consisting of N elements. As the effect of mutual coupling among the elements is ignored, the ideal array factor is

$$AF = \sum_{n=1}^{N} w_n \exp\left[jk\left(ux_n + vy_n\right)\right] \tag{1}$$

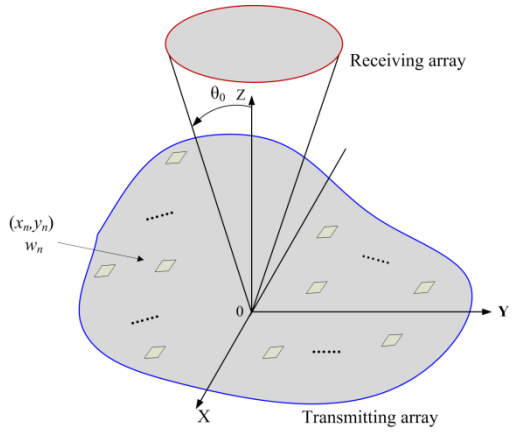

FIGURE 1. Geometry of MPT system.

where w_n and (x_n, y_n) are, respectively, the complex excitation weight and position of nth element. $k = 2\pi/\lambda$ denotes the wave number, $u = \sin\theta\cos\varphi$, and $v = \sin\theta\sin\varphi$. Suppose that the receiving array is in the far region, *BCE* can be expressed as

$$BCE = \frac{\int_{\Psi} |\mathrm{AF}|^2 \, \mathrm{d}\Psi}{\int_{\Omega} |\mathrm{AF}|^2 \, \mathrm{d}\Omega} = \frac{\mathbf{w}\mathbf{R}\mathbf{w}^H}{\mathbf{w}\mathbf{T}\mathbf{w}^H} \tag{2}$$

where Ψ is the receiving region, Ω is the whole visible range of transmitting array, $\mathbf{w}=[w_1, w_2, \ldots, w_N]$, $\mathbf{R}$ and $\mathbf{T}$ are both $N\times N$ matrixes, and superscript "^{H}" stands for transpose and complex-conjugate. The elements of $\mathbf{R}$ and $\mathbf{T}$ are calculated as discussed in [9].

$$R_{mn} = \int_{\Psi} \exp\left[jk\left(u\Delta x_{mn} + v\Delta y_{mn}\right)\right] \mathrm{d}\Psi \tag{3}$$

$$T_{mn} = 4\pi \, \mathrm{sinc}\left(k\sqrt{\Delta x_{mn}^2 + \Delta y_{mn}^2}\right) \tag{4}$$

where $\Delta x_{mn} = x_m - x_n$, and $\Delta y_{mn} = y_m - y_n$. BCE^{opt} is the maximum eigenvalue of the generalized eigenvalue problem [9]

$$\mathbf{R}\mathbf{w}^{\mathrm{opt}} = BCE^{\mathrm{opt}}\mathbf{T}\mathbf{w}^{\mathrm{opt}} \tag{5}$$

in which $\mathbf{w}^{\mathrm{opt}}$ is the corresponding eigenvector. Considering the excitation amplitude and phase errors caused by mechanical and electrical errors, the array factor becomes

$$AF = \sum_{n=1}^{N} A_n\left(1+\delta_n\right)\exp\left[j\varphi_n + jk\left(ux_n + vy_n\right) + j\phi_n\right] \tag{6}$$

where A_n and φ_n are, respectively, the amplitude and phase of complex excitation w_n. The symbol δ_n denotes the amplitude error in percent, and Φ_n represents the phase error. Therefore, the microwave power flowing through the angular region $S = \{\Psi, \Omega\}$ is

$$P^S = \sum_{m=1}^{N}\sum_{n=1}^{N} a_{mn}\delta_{mn}s_{mn}\exp\left[j\Delta\phi_{mn}\right] \tag{7}$$

$$s_{mn} = \int_{S} \exp\left[jk\left(u\Delta x_{mn} + v\Delta y_{mn}\right) + j\Delta\varphi_{mn}\right] \mathrm{d}S \tag{8}$$

where $a_{mn} = A_mA_n$, $\delta_{mn} = (1+\delta_m)(1+\delta_n)$, $\Delta\phi_{mn} = \phi_m - \phi_n$, and $\Delta\varphi_{mn} = \varphi_m - \varphi_n$. It's obvious to find that $s_{mn} = s_{nm}^*$, in which "$*$" stands for complex-conjugate. Assume that δ_n and Φ_n are statistically independent and have a normal distribution with zero mean and standard deviation σ_δ and σ_Φ, respectively, it turns out that (see the Appendix A)

$$P^S = \sum_{m=1}^{N}\sum_{n=1}^{N} a_{mn}\tau_{mn}^S\left(1 + 2\delta_m + \delta_m\delta_n\right) \tag{9}$$

where $\tau_{mn}^S = s_{mn}^r\cos(\Delta\phi_{mn}) - s_{mn}^i\sin(\Delta\phi_{mn})$, s_{mn}^r and s_{mn}^i are the real and imaginary part of s_{mn}, respectively, and $\tau_{mn}^S = \tau_{nm}^S$. According to Taylor polynomial approximation, we can get $\cos(\Delta\phi_{mn}) \approx 1 - \phi_m^2/2 - \phi_n^2/2 + \phi_m\phi_n$ and $\sin(\Delta\phi_{mn}) \approx \phi_m - \phi_n$. By substituting the above two formulas in (9), P^S turns out to be the sum of P_{A}^S and P_{B}^S, the expresses of which are (see the Appendix B)

$$P_{\mathrm{A}}^S = \sum_{m=1}^{N} P_{\mathrm{A}m}^{\mathrm{S}} \tag{10}$$

$$P_{\mathrm{B}}^S = \sum_{m=1}^{N} P_{\mathrm{B}m}^{\mathrm{S}} \tag{11}$$

where $P^S_{\mathrm{A}m} = c^S_{\mathrm{A}m}(1+2\delta_m) - \phi_m(1+\delta_m)(c^S_{\mathrm{B}m}\phi_m + 2c^S_{\mathrm{C}m}) + c^S_{\mathrm{D}m}\delta_m^2$, and $P^S_{\mathrm{B}m} = \delta_m v^S_{\mathrm{A}m} + \phi_m v^S_{\mathrm{B}m} + \delta_m\phi_m v^S_{\mathrm{C}m} + \phi_m^2 v^S_{\mathrm{D}m}$. The coefficients in $P^S_{\mathrm{A}m}$ are given as

$$c^S_{\mathrm{A}m} = \sum_{n=1}^{N} a_{mn}s^r_{mn} \tag{12}$$

$$c^S_{\mathrm{B}m} = \sum_{\substack{n=1\\n\neq m}}^{N} a_{mn}s^r_{mn} \tag{13}$$

$$c^S_{\mathrm{C}m} = \sum_{\substack{n=1\\n\neq m}}^{N} a_{mn}s^i_{mn} \tag{14}$$

$$c^S_{\mathrm{D}m} = a_{mm}s^r_{mm} \tag{15}$$

and the coefficients in $P^S_{\mathrm{B}m}$ are

$$v^S_{\mathrm{A}m} = \sum_{\substack{n=1\\n\neq m}}^{N}\left[a_{mn}s^r_{mn}\delta_n\left(1-\phi_n^2\right) + a_{mn}s^i_{mn}2\phi_n(1+\delta_n)\right] \tag{16}$$

$$v^S_{\mathrm{B}m} = \sum_{\substack{n=1\\n\neq m}}^{N} a_{mn}s^r_{mn}\phi_n \tag{17}$$

$$v^S_{\mathrm{C}m} = \sum_{\substack{n=1\\n\neq m}}^{N} a_{mn}s^r_{mn}(2+\delta_n)\phi_n \tag{18}$$

$$v^S_{\mathrm{D}m} = -\sum_{\substack{n=1\\n\neq m}}^{N} a_{mn}s^r_{mn}\delta_n \tag{19}$$

Thus BCE can be expressed as $BCE = (\eta + P^\Psi_{\mathrm{B}}/P^\Omega_{\mathrm{A}})/(1 + P^\Omega_{\mathrm{B}}/P^\Omega_{\mathrm{A}})$, in which P^Ψ is the receiving power, P^Ω is the total transmitting power, and $\eta = P^\Psi_{\mathrm{A}}/P^\Omega_{A}$. In order to get the upper and lower bounds of BCE, the bounds of η, P^S_{A} and P^S_{B} should be obtained in advance.

B. BOUNDS OF $P^S_{\mathrm{A}}(S = \{\Psi, \Omega\})$ AND η

The mean of $P^S_{\mathrm{A}m}$ is $u^S_{\mathrm{A}m} = c^S_{\mathrm{A}m} - \sigma^2_\Phi c^S_{\mathrm{B}m} + \sigma^2_\delta c^S_{\mathrm{D}m}$, and the variance is $(\sigma^S_{\mathrm{A}m})^2 = \sigma^2_\delta(2c^S_{\mathrm{A}m} - \sigma^2_\Phi c^S_{\mathrm{B}m})^2 + 2\sigma^2_\Phi(1+\sigma^2_\delta)[\sigma^2_\Phi(c^S_{\mathrm{B}m})^2 + 2(c^S_{\mathrm{C}m})^2] + 2\sigma^4_\delta(c^S_{\mathrm{D}m})^2$. Since $P^S_{\mathrm{A}n}$ and $P^S_{\mathrm{A}m}$ $(m \neq n)$ are statistically independent, the mean and variance of P^S_{A} can be got as

$$u^S_{\mathrm{A}} = \sum_{m=1}^{N} u^S_{\mathrm{A}m} \tag{20}$$

$$\left(\sigma^S_{\mathrm{A}}\right)^2 = \sum_{m=1}^{N}\left(\sigma^S_{\mathrm{A}m}\right)^2 \tag{21}$$

and the correlation coefficient between P^Ψ_{A} and P^Ω_{A} is

$$\rho = \sum_{m=1}^{N}\rho_m \tag{22}$$

where $\rho_m = [\sigma^2_\delta(2c^\Psi_{\mathrm{A}m} - \sigma^2_\Phi c^\Psi_{\mathrm{B}m})(2c^\Omega_{\mathrm{A}m} - \sigma^2_\Phi c^\Omega_{\mathrm{B}m}) + 2\sigma^2_\Phi(1+\sigma^2_\delta)(\sigma^2_\Phi c^\Psi_{\mathrm{B}m}c^\Omega_{\mathrm{B}m} + 2c^\Psi_{\mathrm{C}m}c^\Omega_{\mathrm{C}m}) + 2\sigma^4_\delta c^\Psi_{\mathrm{D}m}c^\Omega_{\mathrm{D}m}]/\sigma^\Psi_{\mathrm{A}}\sigma^\Omega_{\mathrm{A}}$. We define L^S as

$$L^S = \frac{1}{\left(\sigma^S_{\mathrm{A}}\right)^4}\sum_{m=1}^{N}\mathrm{E}\left[\left|P^S_{\mathrm{A}m} - u^S_{\mathrm{A}m}\right|^4\right] \tag{23}$$

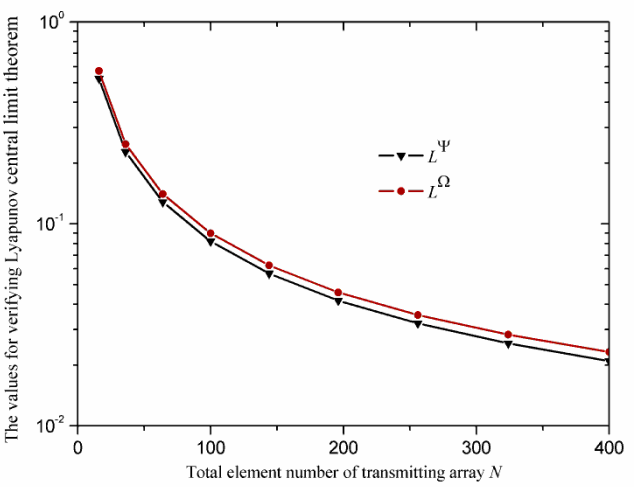

FIGURE 2. L^S for Verifying Lyapunov central limit theorem.

where E() returns the expected value. The values of L^S are shown in Fig. 2. In the calculation process, MPT system has a square transmitting array displaced on a regular lattice of $L_n \times L_n$ and a circular receiving region ($u^2 + v^2 \leq r_0^2$ and $r_0 = 2/L_n$). The complex excitations are set as $\mathbf{w}^{\mathrm{opt}}$ in [9]. As a result, the limit of L^S as N approaches infinity is zero. According to Lyapunov central limit theorem (CLT), P^S_{A} becomes a normal distribution. For the confidence level γ, the confidence interval is $[u^S_{\mathrm{A}} - \beta_1\sigma^S_{\mathrm{A}}, u^S_{\mathrm{A}} + \beta_1\sigma^S_{\mathrm{A}}]$. Namely, the probability that P^S_{A} lay within the interval is equal to γ. For example, β_1=1.96 when γ=95%. Thus the lower bound $(P^S_{\mathrm{A}})^{\mathrm{L}}$ is $u^S_{\mathrm{A}} - \beta_1\sigma^S_{\mathrm{A}}$ and the upper bound $(P^S_{\mathrm{A}})^{\mathrm{U}}$ is $u^S_{\mathrm{A}} + \beta_1\sigma^S_{\mathrm{A}}$.

The bounds of η are related to the correlation coefficient. If $\rho = \pm 1$, which indicates a linear relationship between P^Ψ_{A} and P^Ω_{A}, it turns out that $P^\Psi_{\mathrm{A}} = aP^\Omega_{\mathrm{A}} + b$, $a = \sigma^\Psi_{\mathrm{A}}/\sigma^\Omega_{\mathrm{A}}$, and $b = u^\Psi_{\mathrm{A}} - au^\Omega_{\mathrm{A}}$. Then η can be rewritten as $\eta = a + b/P^\Omega_{\mathrm{A}}$. With the bounds of P^S_{A}, we can get $\eta_1 = \mathrm{a} + \mathrm{b}/(P^\Omega_{\mathrm{A}})^{\mathrm{L}}$ and $\eta_2 = \mathrm{a} + \mathrm{b}/(P^\Omega_{\mathrm{A}})^{\mathrm{U}}$. So the lower bound $\eta^{\mathrm{L}} = \min(\eta_1, \eta_2)$ and the upper bound $\eta^{\mathrm{L}} = \max(\eta_1, \eta_2)$, where min() returns the smaller element and max() returns the larger element. If $\rho \neq \pm 1$, the joint probability density function of P^Ψ_{A} and P^Ω_{A} is

$$f_1\left(P^\Psi_{\mathrm{A}}, P^\Omega_{\mathrm{A}}\right) = \frac{1}{2\pi\sigma^\Psi_{\mathrm{A}}\sigma^\Omega_{\mathrm{A}}\sqrt{1-\rho^2}}\exp\left\{-\frac{1}{2\left(1-\rho^2\right)}\cdot\left[\frac{\left(P^\Psi_{\mathrm{A}} - u^\Psi_{\mathrm{A}}\right)^2}{2\left(\sigma^\Psi_{\mathrm{A}}\right)^2} + \frac{\left(P^\Omega_{\mathrm{A}} - u^\Omega_{\mathrm{A}}\right)^2}{2\left(\sigma^\Omega_{\mathrm{A}}\right)^2} - 2\rho\frac{\left(P^\Psi_{\mathrm{A}} - u^\Psi_{\mathrm{A}}\right)\left(P^\Omega_{\mathrm{A}} - u^\Omega_{\mathrm{A}}\right)}{\sigma^\Psi_{\mathrm{A}}\sigma^\Omega_{\mathrm{A}}}\right]\right\} \tag{24}$$

then the probability density function of η is

$$f_2(\eta) = \int_0^{+\infty} f_1\left(P_{\mathrm{A}}^{\Omega}, P_{\mathrm{A}}^{\Omega}\eta\right) P_{\mathrm{A}}^{\Omega} \mathrm{d}\left(P_{\mathrm{A}}^{\Omega}\right) \tag{25}$$

For the same confidence level γ, the bounds of η can be expressed as $[\eta_0 - \beta_2, \eta_0 + \beta_2]$, in which $\eta_0 = \int_0^1 f_2(\eta)\eta d\eta$ and β_2 is the solution of $\gamma = \int_{\eta_0-\beta_2}^{\eta_0+\beta_2} f_2(\eta) d\eta$.

C. BOUNDS OF P_{B}^{S} ($S = \{\Psi, \Omega\}$)

Through the similar discussion of P_{A}^{S}, variables $v_{\mathrm{A}m}^{S}$, $v_{\mathrm{B}m}^{S}$, $v_{\mathrm{C}m}^{S}$, and $v_{\mathrm{D}m}^{S}$ are all found to be normal distributions with zero means. Their variances are, respectively, $(\sigma_{1m}^{S})^2 = \sigma_\delta^2(3\sigma_\Phi^4 - 2\sigma_\Phi^2 + 1)(\kappa_m^S)^2 + 4(1+\sigma_\delta^2)\sigma_\Phi^2(\vartheta_m^S)^2$, $(\sigma_{2m}^{S})^2 = \sigma_\Phi^2(\kappa_m^S)^2$, $(\sigma_{3m}^{S})^2 = \sigma_\Phi^2(4+\sigma_\delta^2)(\kappa_m^S)^2$, and $(\sigma_{4m}^{S})^2 = \sigma_\delta^2(\kappa_m^S)^2$, in which

$$\kappa_m^{\mathrm{S}} = \sqrt{\sum_{\substack{n=1 \\ n\neq m}}^{N} a_{mn}^2 \left(s_{mn}^r\right)^2} \tag{26}$$

$$\vartheta_m^{\mathrm{S}} = \sqrt{\sum_{\substack{n=1 \\ n\neq m}}^{N} a_{mn}^2 \left(s_{mn}^i\right)^2} \tag{27}$$

Therefore, the confidence intervals are $[-\beta_1\sigma_{qm}^S, \beta_1\sigma_{qm}^S]$ ($q = 1,2,3,4$) for the confidence level γ. Define p_{B}^S as

$$p_{\mathrm{B}}^{\mathrm{S}} = \beta_1 \sum_{m=1}^{N} p_{\mathrm{B}m}^{\mathrm{S}} \tag{28}$$

where $p_{\mathrm{B}m}^S = \delta_m\sigma_{1m}^S + \phi_m\sigma_{2m}^S + \delta_m\phi_m\sigma_{3m}^S + \phi_m^2\sigma_{4m}^S$, and it is obvious that $|P_{\mathrm{B}}^S| \le |p_{\mathrm{B}}^S|$. By using the Lyapunov CLT again, p_{B}^S is also a normal distribution, the mean and variance of which are, respectively

$$u_{\mathrm{B}}^{\mathrm{S}} = \beta_1\sigma_\delta\sigma_\phi^2 \sum_{m=1}^{N} \kappa_m^{\mathrm{S}} \tag{29}$$

$$\left(\sigma_{\mathrm{B}}^{\mathrm{S}}\right)^2 = \beta_1^2 \sum_{m=1}^{N} \left[\sigma_\delta^2 \left(\sigma_{\mathrm{B}1m}^{\mathrm{S}}\right)^2 + \sigma_\phi^2 \left(\sigma_{\mathrm{B}2m}^{\mathrm{S}}\right)^2 + \sigma_\delta^2\sigma_\phi^2 \left(\sigma_{\mathrm{B}3m}^{\mathrm{S}}\right)^2 + 2\sigma_\phi^4 \left(\sigma_{\mathrm{B}4m}^{\mathrm{S}}\right)^2\right] \tag{30}$$

For the confidence level γ, we can get $|p_{\mathrm{B}}^S| \le u_{\mathrm{B}}^S + \beta_1\sigma_{\mathrm{B}}^S$. Considering the condition $|P_{\mathrm{B}}^S| \le |p_{\mathrm{B}}^S|$, the lower and upper bounds of P_{B}^S are $-u_{\mathrm{B}}^S - \beta_1\sigma_{\mathrm{B}}^S$ and $u_{\mathrm{B}}^S + \beta_1\sigma_{\mathrm{B}}^S$, respectively.

D. BOUNDS OF BCE

Based on the above sections, we can get the upper bound of BCE as $\varsigma^{\mathrm{U}} = [\eta^{\mathrm{U}} + (P_{\mathrm{B}}^{\Psi})^{\mathrm{U}}/(P_{\mathrm{A}}^{\Omega})^{\mathrm{L}}]/[1 + (P_{\mathrm{B}}^{\Omega})^{\mathrm{L}}/(P_{\mathrm{A}}^{\Omega})^{\mathrm{L}}]$ and lower bounds as $\varsigma^{\mathrm{L}} = [\eta^{\mathrm{L}} + (P_{\mathrm{B}}^{\Psi})^{\mathrm{L}}/(P_{\mathrm{A}}^{\Omega})^{\mathrm{L}}]/[1 + (P_{\mathrm{B}}^{\Omega})^{\mathrm{U}}/(P_{\mathrm{A}}^{\Omega})^{\mathrm{L}}]$. By considering the practical situation, the bounds of BCE should be modified as $BCE^{\mathrm{U}} = \min(\varsigma^{\mathrm{U}}, BCE^{\mathrm{opt}})$ and $BCE^{\mathrm{L}} = \max(\varsigma^{\mathrm{L}}, 0)$, respectively, where BCE^{opt} is the optimal BCE.

E. INCLUSION PROPERTY OF SA-BASED BOUNDS

Here, it should be indicated that the proposed SA method is not fully inclusive. Namely, not all possible BCE are analytically included in the SA-based bounds. However, a more accurate interval can be obtained because of this property. The following example is given to explain this feature.

Random variable $X_n (n = 1, 2, \ldots, N)$ is supposed to be distributed normally with mean u_n and variance σ_n^2, and X_m and X_n ($m \neq n$) are statistically independent. Then $Y = X_1 + X_2 + \ldots + X_N$ is also a normal distribution with mean $u_Y = u_1 + \ldots + u_N$ and variance $\sigma_Y^2 = \sigma_1^2 + \ldots + \sigma_N^2$. For the confidence lever γ, the confidence interval of $X_n - u_n$ is $-\beta\sigma_n \le X_n - u_n \le \beta\sigma_n$. Therefore, we can get $-\beta\sigma_p \le Y_n - u_Y \le \beta\sigma_p$ by inequality rules and $-\beta\sigma_Y \le Y_n - u_Y \le \beta\sigma_Y$ by the SA method, in which $\sigma_p = \sigma_1 + \ldots + \sigma_N$ and $\sigma_Y < \sigma_p$. We can get a shorter interval by the SA method.

Then we discuss the probability of $Y_n - u_Y = \pm\beta\sigma_p$, defined by p_e. If $\sigma_1 = \ldots = \sigma_N = \sigma$, $p_e = \exp(-N\beta^2/2)/(2N\pi\sigma^2)^{0.5}$. We give some numerical results with $\sigma = 1$ and $\beta = 3$ for different N. For $N = 10$, $p_e = 3.6\times10^{-21}$; for $N = 20$, $p_e = 7.3\times10^{-41}$. Therefore, $Y_n - u_Y$ is impossible to reach $\pm\beta\sigma_p$, which are not included in the SA-based bounds. As a result, the SA-based bounds are better than the inequality-based bounds.

III. ARRAY SYNTHESIS IN THE PRESENCE OF EXCITATION ERRORS

Array synthesis has been studied in many works without considering random excitation errors which are inevitable in practice and will bring bad influence on the MPT applications. It can be seen from (8) that s_{mn}^i will be zero when all elements are excited in-phase for regular receiving region, such as circular region. This feature is good for decreasing the variances of P_{A}^S and P_{B}^S, and then the deviation of BCE from the designed one will be reduced. So, antenna elements are considered to be in-phase in the following discussion.

In this paper, the positions and the nominal excitation amplitudes of antenna elements are optimized simultaneously by using CCDE algorithm to improve the worst performance BCE^{L} of transmitting array based on the proposed SA method. The positions and excitation amplitudes are supposed to be symmetrical about the x-axis and the y-axis, which could reduce the complexity of feed network and the problem dimensions. The optimization model can be established as

$$\text{Find } [x_1, \ldots, x_{N_1}, y_1, \ldots, y_{N_1}, A_1, \ldots, A_{N_1}] \tag{31}$$

$$\text{Max} \cdot f = BCE^L \tag{32}$$

where $N_1 = N/4$. Variables x_n, y_n and $A_n (n = 1, 2, \ldots, N_1)$ are the x position, y position and excitation amplitude of nth element in the first quadrant. The element spacing is constrained by $\Delta x_{mn}^2 + \Delta y_{mn}^2 \ge d_{\min}^2 (m \neq n)$, $x_n \ge d_{\min}/2$ and $y_n \ge d_{\min}/2$, in which $d_{\min}$ is the minimum spacing between adjacent elements. Moreover, all elements are confined on a $D_x \times D_y$ aperture, which can be guaranteed by $x_n \le D_x/2$ and

$y_n \le D_y/2$. In order to deal with the minimum element spacing constraint in computer program, the three steps are carried out. Firstly, random positions are generated for each element by evolutionary algorithm. Secondly, we get the distances between each position and find all unreasonable distances which are less than $d_{\min}$. Thirdly, a penalty according to these unreasonable distances is added to the fitness function (32).

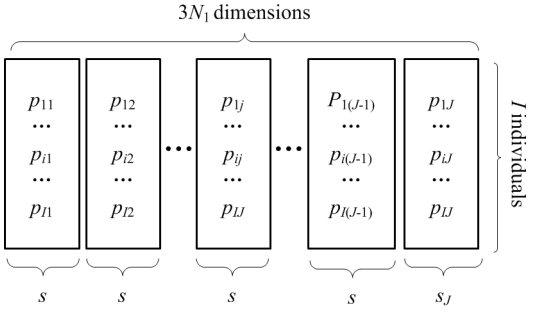

FIGURE 3. Subpopulations in CCDE algorithm.

CCDE algorithm, namely the combination of cooperatively coevolving algorithm and differential evolution algorithm, is used to solve the large-scale optimization problem. The S_K strategy in [21] is considered. As shown in Fig. 3, the $3N_1$ dimensional population with I individuals is decomposed into J subpopulations. The ith individual is denoted as p_i $(i = 1, 2, \ldots, I)$, and the jth part of p_i is denoted as $p_{ij}(i = 1, 2, \ldots, I$, and $j = 1, 2, \ldots, J)$, which is s_j dimensional. In most cases, $s_1 = s_2 = \ldots = s_{J-1} = s$ and $0 < s_J < s$ $(3N_1 = (J-1)s + s_J)$.

The CCDE algorithm will work better if interacting variables are placed within the same subpopulation. However, it is not always known in advance how these $3N_1$ variables are related. To alleviate this problem, we adopt the random grouping structure as proposed in [22]. By randomly decompose the $3N_1$ dimensional population into J subpopulations at each iteration, the probability of placing two interacting variables into the same subpopulation becomes higher and higher over an increasing number of iterations. The pseudocode of CCDE algorithm is given as

Algorithm 1 Create and Initialize J Subpopulations

```
while termination criterion is not met do
    for each subpopulation j = 1, 2, ..., J do
        for each individual i = 1, 2, ..., I do
            if f(com(p_ij, p_i^best)) > f(p_i^best) then
            replace the ith part of p_i^best by p_ij;
            if f(p^best_i) > f(p^best) then
            replace the p^best by p_i^best;
        end for
    end for
    Mutation operation;
    Crossover operation;
end while
```

where $p_i^{\text{best}} = (p_{i1}^{\text{best}}, \ldots, p_{ij}^{\text{best}}, \ldots, p_{iJ}^{\text{best}})$ is the optimal individual over the history of p_i, p_{ij}^{best} is the jth part of p_i^{best}, and p^{best} is the optimal individual of the population over the iterations. The operator com$(p_{ij}, p_i^{\text{best}})$ returns $(p_{i1}^{\text{best}}, \ldots, p_{i(j-1)}^{\text{best}}), p_{ij}, p_{i(j+1)}^{\text{best}}), \ldots, p_{iJ}^{\text{best}})$, and f is the fitness function given as (32).

Here, we adopt DE/Rand/1 strategy in the mutation operation. Then a mutated individual v_i can be generated as

$$v_i(t+1) = p_{r_1}(t) + F[p_{r_2}(t) - p_{r_3}(t)] \tag{33}$$

where t is the current iteration time, r_1, r_2 and r_3 are three random integrals selected from $\{1, 2, \ldots, I\}$, and $r_1 \ne r_2 \ne r_3$. The parameter F is a scaling factor within [0,1]. Then the trial individual u_i is generated by

$$u_{ij}(t+1) = \begin{cases} v_{ij}(t+1), & \text{if rand}() \le C_R \\ p_{ij}(t+1), & \text{otherwise} \end{cases} \tag{34}$$

where rand() returns a random decimal between 0 and 1, and C_R is the crossover probability. The unchanged time of p^{best} is used as a convergence criterion. When p^{best} is not changed above 100 iterations, we should stop the CCDE algorithm.

IV. NUMERICAL RESULTS

In this section, we analyze the tolerance of *BCE* against excitation errors by computer program. Next, we give analysis results of an unequal spacing transmitting array.

A. TOLERANCE ANALYSIS

The validity of the proposed SA method is verified in advance. Accordingly, the minimum confidence level γ is discussed. And then a set of numerical results are provided for different excitation errors and for transmitting arrays different in size. Without loss of generality, MPT system is supposed to have a square transmitting array of $L_n \times L_n$ positions and a square receiving region $(-u_0 \le u \le u_0, -v_0 \le v \le v_0)$. The excitation weights across transmitting array are set as $\mathbf{w}^{\text{opt}}$ [9] which is corresponding to the BCE^{opt}.

Provided that $u_0 = v_0 = 0.2$ and $L_n = 10$, BCE^{opt} is 95.4% which agrees well with the result achieved in [9] ($BCE = 96.45\%$). The following two error cases are considered: $(\sigma_\delta, \sigma_\Phi) = (0.05, 5^\circ)$ and $(\sigma_\delta, \sigma_\Phi) = (0.1, 10^\circ)$. For a preliminary verification, $Q = 10^5$ different random excitation errors corresponding to $(\sigma_\delta, \sigma_\Phi)$ have been generated. Hence every $BCE^q (q = 1, 2, 3 \ldots, Q)$ can be calculated. When $\gamma = 99.9\%$, the SA-based bounds of *BCE* are [92.0%,95.4%] and [81.7%,95.4%], respectively. As shown in Fig. 4, the fact that all BCE^q are within the SA-based bounds fully confirms the validity of the proposed SA method.

The bounds of *BCE* are directly related to the confidence level γ. To discuss about the minimum γ, the width of *BCE* is denoted as $\Delta BCE = BCE^{\text{U}} - BCE^{\text{L}}$ and the probability that BCE^q lay within the SA-bounds is denoted as p_{in}. The numerical results of different γ are shown in Fig. 5 for

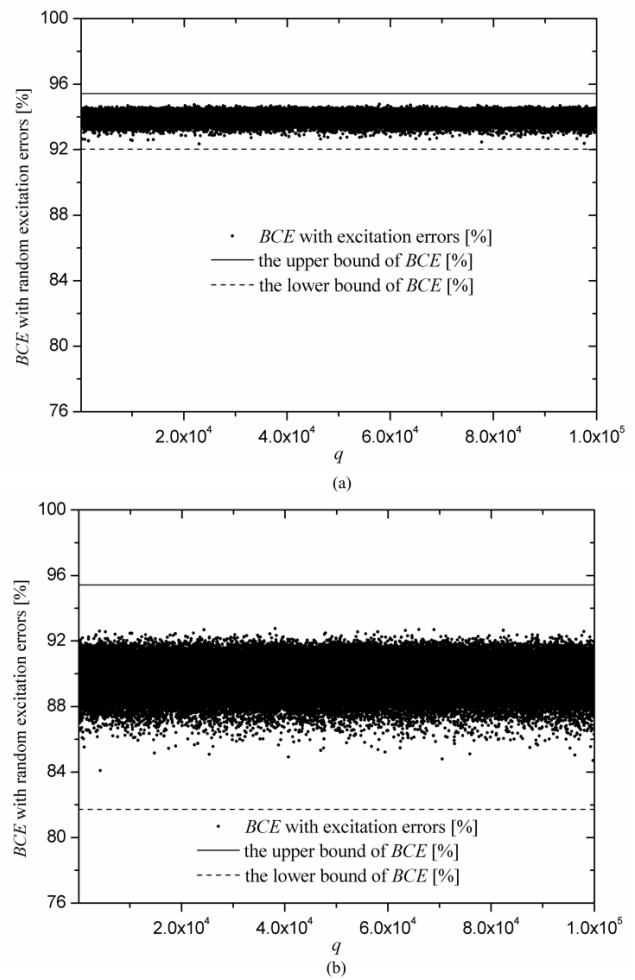

FIGURE 4. BCE with random excitation errors and the SA-based bounds. (a) $(\sigma_\delta, \sigma_\Phi) = (0.05, 5°)$. (b) $(\sigma_\delta, \sigma_\Phi) = (0.1, 10°)$.

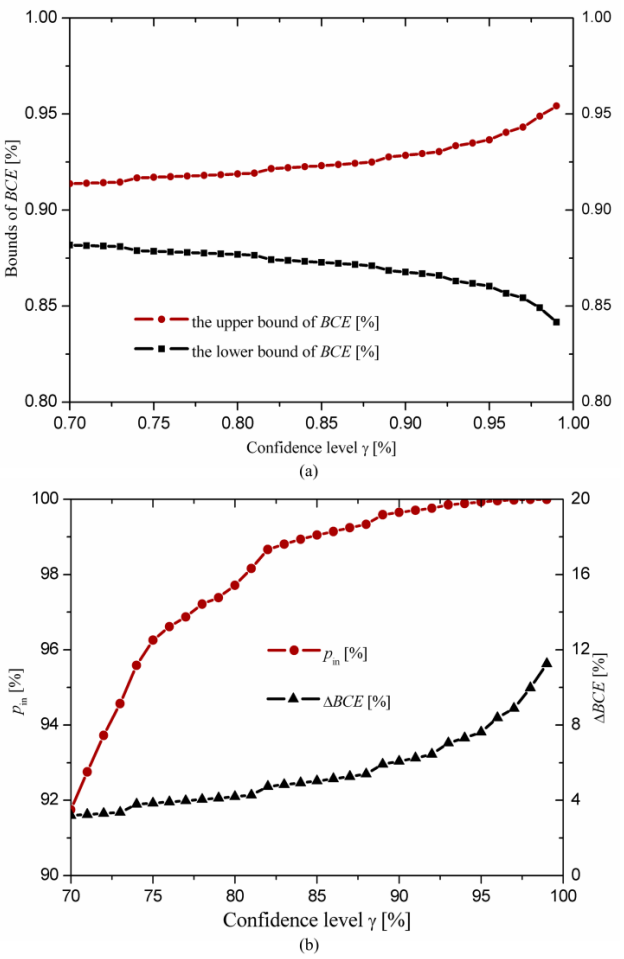

FIGURE 5. Effect of confidence level γ. (a) on the bounds of BCE. (b) on p_{in} and ΔBCE.

$(\sigma_\delta, \sigma_\Phi) = (0.1, 10°)$. As γ increases, BCE^{U} increases and BCE^{L} decreases. Therefore, p_{in} gradually increases due to the larger ΔBCE. The results show that γ should be larger than 97% to guarantee $p^{\mathrm{in}} \geq 99.9\%$.

Numerical results for different excitation errors are shown in Fig. 6 with $\gamma = 97\%$. The maximum deviation of $BCE$from the optimal one BCE^{opt} is defined as $d_{BCE} = BCE^{\mathrm{L}} - BCE^{\mathrm{opt}}$, which indicates the worst performance of transmitting array. Obviously, BCE^{L} and BCE^{U} both decrease when σ_δ or σ_Φ increases. As a result, d_{BCE} increases to 12.6%. With these results, we can do some preliminary predication. For example, σ_δ should not be larger than 0.07 for the case of $\sigma_\Phi = 5°$ if the deviation is confined by $d_{BCE} < 3\%$.

The next example is concerned with arrays different in element number (corresponding to L_n). In order to eliminate the effects of other factors, the BCE^{opt} is constrained to be 95%. The receiving region parameters u_0 and v_0 are decided by a bisection method to guarantee the BCE of 95%. With $(\sigma_\delta, \sigma_\Phi)$ is fixed as $(0.1, 10°)$, numerical results are shown in Fig. 7. It can be seen that the deviation of BCE decreases from 11.8% to 8.7% when the element number varies from 36 to 400. As a result, we can reduce the impact of random excitation errors by increasing the element number of transmitting array.

B. ARRAY SYNTHESIS

The unequal spacing planar array (100 elements) in [14] is considered as a reference array, because it has a BCE of 89.96% which is 3.5% higher than the optimal one in [9] ($BCE^{\mathrm{opt}} = 86.48\%$). The receiving region is a circular one ($u^2 + v^2 \leq r_0^2$ and $r_0 = 0.2$). However, the BCE^{L} is 81.1% for the excitation errors $(\sigma_\delta, \sigma_\Phi) = (0.1, 10°)$, which is 8.9% lower than the designed one. Based on the SA-CCDE algorithm, the positions and nominal excitation amplitudes are optimized simultaneous to improve BCE^{L}. The minimum spacing between adjacent elements $d_{\min}$ is 0.4λ, and the maximum aperture size is $4.5\lambda \times 4.5\lambda$. As a result, the BCE^{L} is improved by 3.8% from 81.1% to 84.9%. That means we can guarantee BCE of 84.9% in the presence of excitation errors $(\sigma_\delta, \sigma_\Phi) = (0.1, 10°)$. The corresponding positions and nominal excitation amplitudes are shown in Fig. 8. The circles indicate element positions, and the values in circles denote the nominal excitation amplitudes.

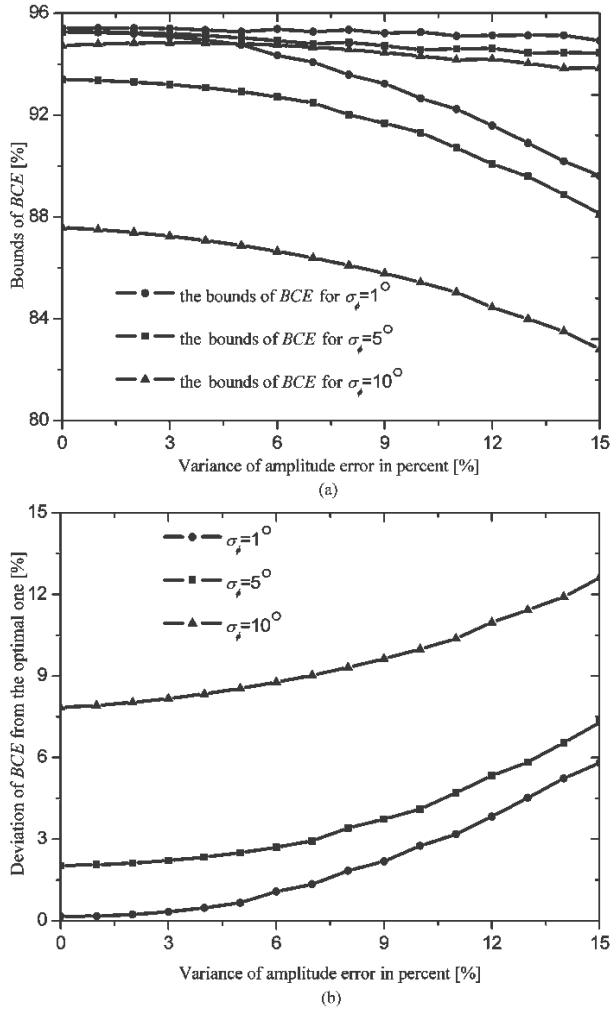

FIGURE 6. Effect of different excitation errors. (a) on the bounds of *BCE*. (b) on deviation of *BCE* from the optimal one.

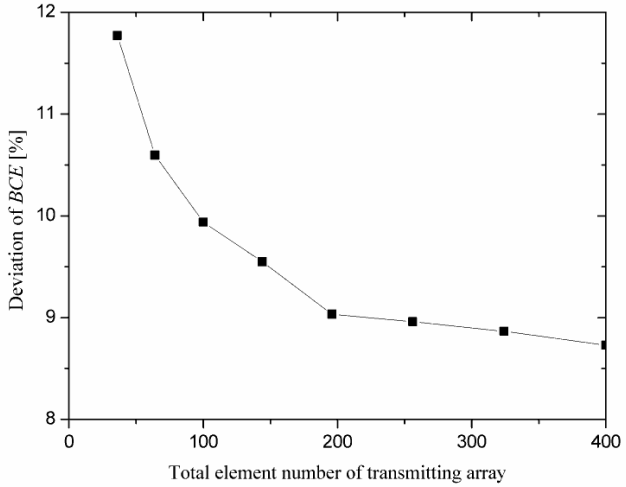

FIGURE 7. The deviation of *BCE* for different size transmitting array.

In the next example, the elements are confined on a $6\lambda \times 6\lambda$ aperture, while the element number, the minimum element spacing and the receiving region are not changed.

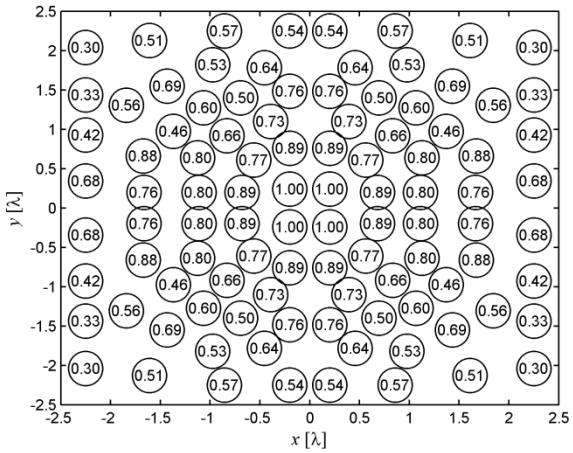

FIGURE 8. The optimized element positions and excitation amplitudes for $4.5\lambda \times 4.5\lambda$ transmitting aperture.

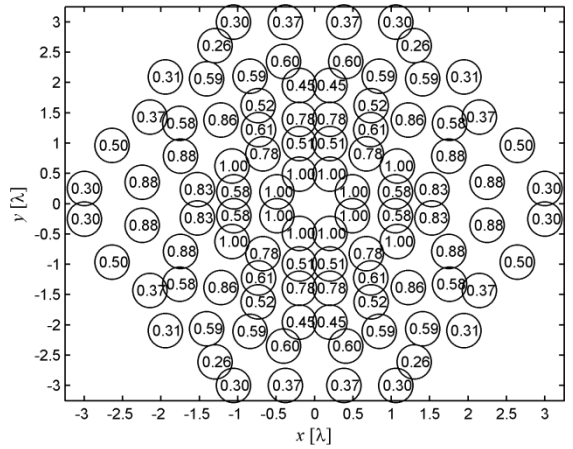

FIGURE 9. The optimized element positions and excitation amplitudes for $6\lambda \times 6\lambda$ transmitting aperture.

The optimized positions and nominal excitation amplitudes are shown in Fig. 9. The BCE^{L} is improved by 4% from 81.1% to 85.1%, which is close to the one of $4.5\lambda \times 4.5\lambda$ transmitting aperture. From the two optimized array and the numerical results of tolerance analysis, we can find that the BCE^{L} is sensitive to the element number, not the aperture size.

V. CONCLUSION

In this paper, a SA method is presented to evaluate the achievable *BCE* in the presence of excitation errors. Then based on the worst *BCE* obtained by the SA method, we propose a synthesis method of transmitting array for optimal MPT by using CCDE algorithm. The tolerance of *BCE* against the random excitation errors is simulated by computer program, and the positions and nominal excitation amplitudes are both simultaneously optimized to improve the worst *BCE*. Numerical results indicate the validity of the SA method, and show that the worst *BCE* is improved about 4% from 81% to 85% based on the SA-CCDE synthesis method for the excitation errors $(\sigma_\delta, \sigma_\Phi) = (0.1, 10)$.

APPENDIX A
DERIVATION OF (9)

With $a_{mn} = a_{nm}$, $\delta_{mn} = \delta_{nm}$, $\Delta\phi_{mn} = -\Delta\phi_{nm}$, and $s_{mn} = s_{nm}^*$, (7) can be rewritten as

$$\begin{aligned} P^S &= \sum_{m=1}^{N}\sum_{n=m+1}^{N} a_{mn}\delta_{mn}\left[s_{mn}\exp\left(j\Delta\phi_{mn}\right)\right. \\ &\quad \left. + s_{mn}^*\exp\left(-j\Delta\phi_{mn}\right)\right] + \sum_{m=1}^{N} a_{mm}\delta_{mm}s_{mm} \\ &= 2\sum_{m=1}^{N}\sum_{n=m+1}^{N} a_{mn}\delta_{mn}\left[s_{mn}^r\cos\left(\Delta\phi_{mn}\right)\right. \\ &\quad \left. - s_{mn}^i\sin\left(\Delta\phi_{mn}\right)\right] + \sum_{m=1}^{N} a_{mm}\delta_{mm}s_{mm} \end{aligned} \tag{35}$$

Due to $s_{mm} = s_{mm}^r$, P^S can be expressed as

$$P^S = \sum_{m=1}^{N}\sum_{n=1}^{N} a_{mn}\delta_{mn}\left[s_{mn}^r\cos\left(\Delta\phi_{mn}\right) - s_{mn}^i\sin\left(\Delta\phi_{mn}\right)\right] \tag{36}$$

so

$$P^S = \sum_{m=1}^{N}\sum_{n=1}^{N} a_{mn}\tau_{mn}^S\left(1+\delta_m+\delta_n+\delta_m\delta_n\right) \tag{37}$$

With $\tau_{mn}^S = \tau_{nm}^S$, the third part of P^S can be transformed as

$$\sum_{m=1}^{N}\sum_{n=1}^{N} a_{mn}\tau_{mn}^S\delta_n = \sum_{m=1}^{N}\sum_{n=1}^{N} a_{nm}\tau_{nm}^S\delta_m = \sum_{m=1}^{N}\sum_{n=1}^{N} a_{mn}\tau_{mn}^S\delta_m \tag{38}$$

The transform method will be used many times in the following Appendix B. Substituting (38) in (37), (9) can be obtained.

APPENDIX B
DERIVATION OF P_{A}^S and P_{B}^S

With the taylor polynomial approximation of $\cos(\Delta\phi_{mn})$ and $\sin(\Delta\phi_{mn})$, (9) can be expanded as

$$\begin{aligned} P^S &= \sum_{m=1}^{N}\sum_{n=1}^{N} a_{mn}s_{mn}^r\left(1+\delta_m\delta_n\right)\left(1-\frac{1}{2}\phi_m^2-\frac{1}{2}\phi_n^2+\phi_m\phi_n\right) \\ &\quad + \sum_{m=1}^{N}\sum_{n=1}^{N} a_{mn}s_{mn}^r\delta_m\left(2-\phi_m^2-\phi_n^2+2\phi_m\phi_n\right) \\ &\quad - \sum_{m=1}^{N}\sum_{n=1}^{N} a_{mn}s_{mn}^i\left(1+\delta_m\delta_n\right)\left(\phi_m-\phi_n\right) \\ &\quad - \sum_{m=1}^{N}\sum_{n=1}^{N} a_{mn}s_{mn}^i 2\delta_m\left(\phi_m-\phi_n\right) \end{aligned} \tag{39}$$

P^S turns out to be as follow by using transform method in (38).

$$\begin{aligned} P^S &= \sum_{m=1}^{N}\sum_{n=1}^{N} a_{mn}s_{mn}^r\left(1+\delta_m\delta_n\right)\left(1-\phi_m^2+\phi_m\phi_n\right) \\ &\quad + \sum_{m=1}^{N}\sum_{n=1}^{N} a_{mn}s_{mn}^r\delta_m\left(2-\phi_m^2-\phi_n^2+2\phi_m\phi_n\right) \\ &\quad - \sum_{m=1}^{N}\sum_{n=1}^{N} a_{mn}s_{mn}^i\left(1+\delta_m\delta_n\right)2\phi_m \\ &\quad - \sum_{m=1}^{N}\sum_{n=1}^{N} a_{mn}s_{mn}^i 2\delta_m\left(\phi_m-\phi_n\right) \end{aligned} \tag{40}$$

Therefore, the two parts of P^S are

$$\begin{aligned} P_{\mathrm{A}}^S &= \sum_{m=1}^{N}\sum_{n=1}^{N} a_{mn}s_{mn}^r\left(1-\phi_m^2+2\delta_m-\phi_m^2\delta_m\right) \\ &\quad + \sum_{m=1}^{M} a_{mm}s_{mm}^r\left(\phi_m^2+\delta_m^2+\delta_m\phi_m^2\right) \\ &\quad - \sum_{m=1}^{N}\sum_{n=1}^{N} a_{mn}s_{mn}^i 2\phi_m\left(1+\delta_m\right) \end{aligned} \tag{41}$$

$$\begin{aligned} P_{\mathrm{B}}^S &= \sum_{m=1}^{N}\sum_{\substack{n=1\\n\neq m}}^{N} a_{mn}s_{mn}^r\left(\phi_m\phi_n+\delta_m\delta_n-\delta_m\delta_n\phi_m^2\right) \\ &\quad + \sum_{m=1}^{N}\sum_{\substack{n=1\\n\neq m}}^{N} a_{mn}s_{mn}^r\left(2\delta_m\phi_m\phi_n-\phi_n^2\delta_m+\delta_m\delta_n\phi_m\phi_n\right) \\ &\quad - \sum_{m=1}^{N}\sum_{\substack{n=1\\n\neq m}}^{N} a_{mn}s_{mn}^i 2\delta_m\left(\delta_n\phi_m-\phi_n\right) \end{aligned} \tag{42}$$

For P_{A}^S,

$$\sum_{m=1}^{N}\sum_{n=1}^{N} a_{mn}s_{mn}^r = \sum_{m=1}^{N} c_{\mathrm{A}m}^S \tag{43}$$

$$\sum_{m=1}^{N}\sum_{n=1}^{N} a_{mn}s_{mn}^r 2\delta_m = 2\sum_{m=1}^{N}\delta_m c_{\mathrm{A}m}^S \tag{44}$$

$$\begin{aligned} &- \sum_{m=1}^{N}\sum_{n=1}^{N} a_{mn}s_{mn}^r\phi_m^2 + \sum_{m=1}^{M} a_{mm}s_{mm}^r\phi_m^2 \\ &\quad = -\sum_{m=1}^{N}\phi_m^2 c_{\mathrm{B}m}^S \end{aligned} \tag{45}$$

$$\begin{aligned} &- \sum_{m=1}^{N}\sum_{n=1}^{N} a_{mn}s_{mn}^r\phi_m^2\delta_m + \sum_{m=1}^{M} a_{mm}s_{mm}^r\delta_m\phi_m^2 \\ &\quad = -\sum_{m=1}^{N}\phi_m^2\delta_m c_{\mathrm{B}m}^S \end{aligned} \tag{46}$$

$$-\sum_{m=1}^{N}\sum_{n=1}^{N} a_{mn}s_{mn}^{i}2\phi_m\left(1+\delta_m\right) = -\sum_{m=1}^{N} 2\phi_m\left(1+\delta_m\right)c_{\mathrm{C}m}^{S} \tag{47}$$

$$\sum_{m=1}^{M} a_{mm}s_{mm}^{r}\delta_m^2 = \sum_{m=1}^{N}\delta_m^2 c_{\mathrm{D}m}^{S} \tag{48}$$

Substituting (43)-(48) in (41), we can get (10) where $P_{\mathrm{A}m}^{S} = c_{\mathrm{A}m}^{S}(1+2\delta_m) - \phi_m(1+\delta_m)\left(c_{\mathrm{B}m}^{S}\phi_m + 2c_{\mathrm{C}m}^{S}\right) + c_{\mathrm{D}m}^{S}\delta_m^2$. For P_{B}^{S}, with $s_{mn} = s_{nm}^{*}$, the following three parts of P_{B}^{S} can be expressed as

$$\begin{aligned}\sum_{m=1}^{N}\sum_{\substack{n=1\\n\neq m}}^{N} a_{mn}s_{mn}^{r}\delta_m\delta_n\phi_m^2 &= \sum_{n=1}^{N}\sum_{\substack{m=1\\m\neq n}}^{N} a_{nm}s_{nm}^{r}\delta_n\delta_m\phi_n^2\\ &= \sum_{m=1}^{N}\sum_{\substack{n=1\\n\neq m}}^{N} a_{mn}s_{mn}^{r}\delta_m\delta_n\phi_n^2\end{aligned} \tag{49}$$

$$\sum_{m=1}^{N}\sum_{\substack{n=1\\n\neq m}}^{N} a_{mn}s_{mn}^{r}\phi_n^2\delta_m = \sum_{n=1}^{N}\sum_{\substack{m=1\\m\neq n}}^{N} a_{mn}s_{mn}^{r}\phi_m^2\delta_n \tag{50}$$

$$\sum_{m=1}^{N}\sum_{\substack{n=1\\n\neq m}}^{N} a_{mn}s_{mn}^{r}2\delta_m\phi_m\phi_n = \sum_{m=1}^{N}\sum_{\substack{n=1\\n\neq m}}^{N} a_{mn}s_{mn}^{r}2\delta_n\phi_m\phi_n \tag{51}$$

Substituting (49)-(51) in (42), we can get the final expression of P_{B}^{S}.

REFERENCES

[1] S. Sasaki, K. Tanaka, and K.-I. Maki, "Microwave power transmission technologies for solar power satellites," *Proc. IEEE*, vol. 101, no. 6, pp. 1438–1447, Jun. 2013.

[2] A. Massa, G. Oliveri, F. Viani, and P. Rocca, "Array designs for long-distance wireless power transmission: State-of-the-art and innovative solutions," *Proc. IEEE*, vol. 101, no. 6, pp. 1464–1481, Jun. 2013.

[3] B. Strassner and K. Chang, "Microwave power transmission: Historical milestones and system components," *Proc. IEEE*, vol. 101, no. 6, pp. 1379–1396, Jun. 2013.

[4] H. Sun and W. Geyi, "Optimum design of wireless power transmission systems in unknown electromagnetic environments," *IEEE Access*, vol. 5, pp. 20198–20206, 2017.

[5] R. M. Dickinson and W. C. Brown, "Radiated microwave power transmission system efficiency measurements," Jet Propuls. Lab., California Inst. Technol., Pasadena, CA, USA, Tech. Memo. 33-727, Mar. 1975.

[6] R. M. Dickinson, "Performance of a high-power, 2.388-GHz receiving array in wireless power transmission over 1.54 km," in *IEEE MTT-S Int. Microw. Symp. Dig.*, Jun. 1976, pp. 139–141.

[7] P. Evans. (Feb. 22, 2009). Solar power beamed from space within a decade? Gizmag. [Online]. Available: http://newatlas.com/solar-power-space-satellite/11064/

[8] S. Prasad, "On the index for array optimization and the discrete prolate spheroidal functions," *IEEE Trans. Antennas Propag.*, vol. AP-30, no. 5, pp. 1021–1023, Sep. 1982.

[9] G. Oliveri, L. Poli, and A. Massa, "Maximum efficiency beam synthesis of radiating planar arrays for wireless power transmission," *IEEE Trans. Antennas Propag.*, vol. 61, no. 5, pp. 2490–2499, May 2013.

[10] V. N. Garmash and S. S. Shaposhnikov, "Matrix method synthesis of transmitting antenna for wireless power transmission," *IEEE Trans. Aerosp. Electron. Syst.*, vol. 36, no. 4, pp. 1142–1148, Oct. 2000.

[11] A. K. M. Baki, N. Shinohara, H. Matsumoto, K. Hashimoto, and T. Mitani, "Study of isosceles trapezoidal edge tapered phased array antenna for solar power station/satellite," *IEICE Trans. Commun.*, vol. E90-B, no. 4, pp. 968–977, Apr. 2007.

[12] A. K. M. Baki, K. Hashimoto, N. Shinohara, T. Mitani, and H. Matsumoto, "New and improved method of beam forming with reduced side lobe levels for microwave power transmission," in *Proc. 5th Int. Conf. Electr. Comput. Eng.*, Dhaka, Bangladesh, Dec. 2008, pp. 773–777.

[13] X. Li, B. Duan, L. Song, Y. Zhang, and W. Xu, "Study of stepped amplitude distribution taper for microwave power transmission for SSPS," *IEEE Trans. Antennas Propag.*, vol. 65, no. 10, pp. 5396–5405, Oct. 2017.

[14] X. Li, B. Duan, J. Zhou, L. Song, and Y. Zhang, "Planar array synthesis for optimal microwave power transmission with multiple constraints," *IEEE Antennas Wireless Propag. Lett.*, vol. 16, pp. 70–73, Feb. 2017.

[15] P. Rocca, G. Oliveri, and A. Massa, "Innovative array designs for wireless power transmission," in *Proc. IEEE Int. Microw. Workshop Ser. Innov. Power Transmiss., Technol. Syst. Appl.*, Kyoto, Japan, May 2011, pp. 279–282.

[16] A. F. Morabito, A. R. Laganà, and T. Isernia, "Optimizing power transmission in given target areas in the presence of protection requirements," *IEEE Antennas Wireless Propag. Lett.*, vol. 14, pp. 44–47, 2014.

[17] A. F. Morabito, "Synthesis of maximum-efficiency beam arrays via convex programming and compressive sensing," *IEEE Antennas Wireless Propag. Lett.*, vol. 16, pp. 2404–2407, 2017.

[18] X. Li, J. Z. Zhou, and Y. Q. Zhang, "Performance of planar arrays for microwave power transmission with phase shifter errors," in *Proc. 5th Asia Int. Symp. Mechatron.*, Oct. 2015, p. 4.

[19] X. Li, J. Zhou, B. Duan, Y. Yang, Y. Zhang, and J. Fan, "Performance of planar arrays for microwave power transmission with position errors," *IEEE Antennas Wireless Propag. Lett.*, vol. 14, pp. 1794–1797, Nov. 2015.

[20] C.-H. Chen and W.-H. Chen, "Cooperatively coevolving differential evolution for compensatory neural fuzzy networks," in *Proc. Int. Conf. Fuzzy Theory Appl.*, Dec. 2013, pp. 264–267.

[21] F. van den Bergh and A. P. Engelbrecht, "A cooperative approach to particle swarm optimization," *IEEE Trans. Evol. Comput.*, vol. 8, no. 3, pp. 225–239, Jun. 2004.

[22] Z. Yang, K. Tang, and X. Yao, "Large scale evolutionary optimization using cooperative coevolution," *Inf. Sci.*, vol. 178, no. 15, pp. 2985–2999, 2008.

HUA-WEI ZHOU was born in 1988. He received the B.S. and M.S. degrees from the School of Communication and Information Engineering, Shanghai University, in 2011 and 2013, respectively, where he is currently pursuing the Ph.D. degree. His research interests include microwave power transmission and finite-difference time-domain method.

XUE-XIA YANG was born in 1969. She received the B.S. and M.S. degrees in radio physics from Lanzhou University in 1991, and 1994, respectively, and the Ph.D. degree from the School of Communication and Information Engineering, Shanghai University, in 2001. Since 2008, she has been a Professor and a Doctoral Supervisor with the School of Communication and Information Engineering, Shanghai University. Her areas of research interest include planar antenna design, computational electromagnetics, and microwave power transmission.

SAJJAD RAHIM was born in 1986. He received the bachelor's degree in telecommunication engineering and the M.Sc. degree in telecommunication engineering from the University of Engineering and Technology, Peshawar, in 2009 and 2016, respectively. He is currently pursuing the Ph.D. degree in electromagnetics and microwave engineering with Shanghai University, China. His research interests include MIMO antenna, 5G antenna, and metamaterials.